

Wind tunnel model support and wall interference corrections in DNW-HST

- ensuring high data quality standards

Frenk Wubben

Project manager

Project Aerodynamics

German Dutch Wind Tunnels DNW

E-mail: frenk.wubben@dnw.aero

Edgard Takara

Product Development Engineer

Aeronautics Engineering - Wind Tunnel Testing Team

Embraer - São José dos Campos

E-mail: edgard.takara@embraer.com.br

ABSTRACT

The DNW-HST is a closed-circuit, slotted walls, pressurized transonic wind tunnel facility, used by the industry to support the development of aircraft and launch vehicles at close- to actual flight Reynolds numbers. As part of a continuous effort to increase simulation accuracy, together with the National Aerospace Laboratory (NLR) and Embraer a dedicated project was successfully completed, focusing on further refinement of model support and wall interference corrections.

As part of this joint project, results from other wind tunnel facilities and numerical analyses were applied to verify the improved correction procedures for a rear model support in the DNW-HST. The data is evaluated taking into account wind tunnel instrument uncertainty and uncertainty in Computational Fluid Dynamics (CFD) data. The agreement of the corrected data with results from other wind tunnels appears to be within the experimental instrument uncertainty limits. Differences in lift coefficient are observed between the experimental and CFD results. These differences might be due to inaccuracies in the numerical approach and wing deformation effects in the experimental results.

NOMENCLATURE

Alpha, α	Angle of attack	[deg]
b	Wing span	[m]
Beta, β	Slip angle	[deg]
C	Model chord	[-]
CD	Drag coefficient (wind axis)	[-]
CDNET	$CD-CL^2/(\pi \cdot b^2/S)$	[-]
CL	Lift coefficient (wind axis)	[-]
CLO	Lift coefficient at $\alpha=0$ deg	[-]
CM	Pitching moment coefficient	[-]
Cp	Pressure coefficient	[-]
Ma	Mach number	[-]
Re	Reynolds number	[-]
S	Model reference area	[m ²]
U _m	Model induced normalized axial velocity	[-]
U _t	Total disturbance normalized axial velocity	[-]
U _w	Wall-induced normalized axial velocity	[-]
X _T , Y _T , Z _T	Tunnel axis system	[m]

1 INTRODUCTION

With increasing demands from customers to obtain accurate absolute drag values from transonic wind tunnels, DNW is continuously improving the measurement chain and the wind tunnel corrections i.e. model support and wall interference corrections.

1. The most important source of uncertainty in the measurement chain is the main balance for measuring the aerodynamic coefficients. For this reason, considerable efforts are spent and ongoing at DNW to decrease the uncertainty levels of the main balance instrumentation.
2. The level of support interference corrections is strongly dependent on the adopted test setup. The choice for the model support is a compromise between test productivity, data consistency and support interference level. The effects can be in the order of 10-20% of the minimum drag value. Hence, an accurate correction procedure is necessary to correct for these effects.
3. Wall interference effects are minimized in DNW-HST by the use of slotted upper and lower walls and are in general about one order of magnitude lower than the effects of the model support.

Due to the relative large contribution of the model support in the wind tunnel corrections, a critical review of the support interference correction procedure was performed in 2007. Until that time, not all model support effects were taken into account and hence, the accuracy of the corrections could be improved.

Support interference effects are split in two contributions which are linked to the following model support parts (see figure 1):

1. Near field effect: due to the sting which connects the wind tunnel model to the boom support.
2. Far field effect: due to the support boom for variation of the model angle of attack and side slip angle.

In the support interference procedure that was used up to 2007, the near field effect was corrected in the lift, drag and pitching moment components and was obtained from dummy sting measurements. The far field effect, however, was corrected in the drag component only by a buoyancy correction at zero angle of attack, i.e. the effect of angle of attack was not considered. In addition, no far field correction was applied for lift and pitching moment although significant effects can be present on these components as well. Hence, improvements were possible and necessary, considering the effects of the complete support system on lift, drag and pitching moment. For this reason, dummy support measurements were introduced replacing execution of dummy sting measurements only. CFD calculations performed by the NLR validated the new experimental support interference correction procedure.

Although the new support interference procedure provides more consistent and reliable corrections, the corrected results are not always in agreement with expectations. A possible explanation is that a wall interference effect is acting on the model which was previously - by coincidence - compensated by the errors in the old support interference procedure. Until 2007, a wall interference correction did not seem to be necessary for well-scaled complete wind tunnel models.

Hence, focus was directed to assess the effect of the wind tunnel walls in more detail. The hypothesis is that a wall-induced pressure gradient pushes the model downstream, increasing the measured drag levels. Without correction for this effect, the drag levels are higher than expected. This wall interference effect can be dependent on the streamwise position of the model in the slotted wall test section.

In order to investigate this hypothesis, a cooperative project was started with Embraer, DNW and NLR in 2014. In this project, the entire measurement chain and wind tunnel correction procedures were investigated using verification data from CFD codes (NLR and Embraer) as well as experimental data acquired by Embraer in the European Transonic Wind tunnel (ETW).

2 AIM AND APPROACH

The aim of the project is to improve the absolute accuracy of lift, drag and pitching moment measurement results in the DNW-HST. The focus is on further refinement of corrections for support and wall interference effects.

Support and wall interference effects are determined by experimental means in the DNW-HST wind tunnel. In this experiment, an Embraer wind tunnel model is measured with an internal main balance on existing DNW-HST test setups. We distinguish:

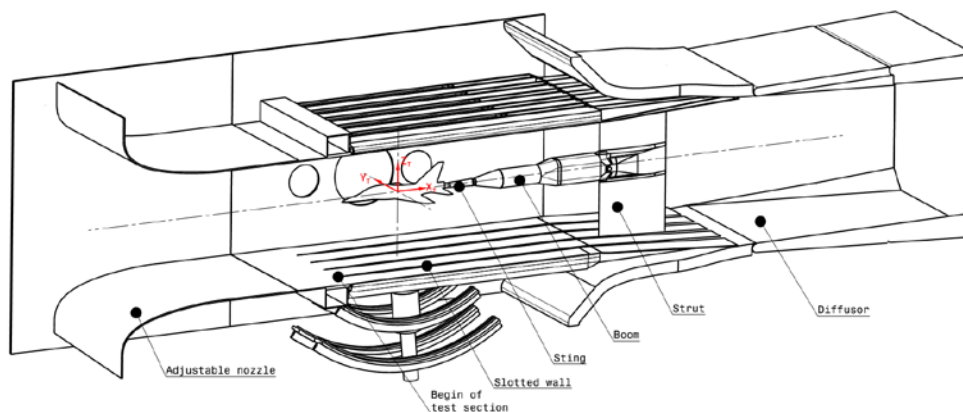
- Production runs, which are performed with the wind tunnel model mounted upside up on a rear support.
- Support interference assessments with the model mounted upside down on a dorsal support. These measurements are performed with and without the presence of a dummy rear support.
- For wall interference assessments, wall pressures are measured during the production runs. In addition, also empty test section wall pressure measurements are performed with only the rear support present in the test section.

It is well known that support and wall interference effects are dependent on lift and Mach number. In order to discriminate between the effects of lift and Mach number, model configurations with and without wings are measured. One of the considered model configurations in the DNW-HST is also measured in the ETW. Results from the ETW and numerical analysis performed by NLR and Embraer are used to verify the data corrected for support and wall interference effects.

3 WIND TUNNEL FACILITY

The experiments are performed in the DNW-HST transonic wind tunnel located in Amsterdam, The Netherlands. The 1.60/1.80 x 2.00 m² DNW-HST is a variable-density closed circuit wind tunnel. An adjustable nozzle is followed by a test section with solid side walls and movable slotted top and bottom walls. Top and bottom walls can be adjusted to obtain a test section height of 1.60 m or 1.80 m. The current test is performed at a tunnel height of 1.80 m.

Figure 1: Schematic view of DNW-HST test section including, nozzle, diffuser and plenum chamber



The test section is surrounded by a plenum chamber to accommodate in- and outflow from the test section slotted walls. The stagnation pressure can be varied between 20 and 390 kPa. The tunnel is calibrated for Mach numbers between 0.20 and 1.30. All four walls are provided with windows and are instrumented with pressure taps. Several model support booms are available, which are mounted to a strut that is movable in vertical position. The origin of the test section axis system is at the center of the main window with positive X_T -axis in stream wise direction and Z_T -axis to the top wall. The beginning of the slotted test section is at $X_T = -1.225$ m.

The test section centerline pressure distribution is calibrated in reference to the plenum pressure, using a long static tube with pressure taps. Calibrations are performed for different model supports at varying Mach numbers. The calibrations are used to set the free stream Mach number and static pressure at the model reference point (MRP). In addition, the calibrated centerline pressure distribution is used to calculate the buoyancy effect of the support boom on the drag component of the wind tunnel model. This buoyancy correction is used as a first estimate of the far field support interference correction on drag.

4 MODEL AND TEST SETUP

The model is designed for forces and moment measurements by means of an internal six-component strain gage balance, manufactured by TASK Corporation. The uncertainty of this 2.5 inch balance is $\pm 0.3\%$ of the full scale of each component. The maximum range in lift is ± 14600 N. Model configurations can be assembled from body-alone to wing-body-nacelle to complete configuration with tail. Laminar to turbulent transition tripping is ensured by using carborundum bands on the fuselage nose, wings, pylon and nacelles, and empennage. The trip size is optimized for a Reynolds number of 3 million based on a model chord of 0.17 m. The model is prepared for measurements on a rear support as well as a dorsal support.

4.1 Rear support

The model on rear sting is mounted to the double roll boom (see figure 2). With this model support, an angle of attack (α) range between -10 and 20 deg is possible and side slip angle (β) range of -10 to 10 deg. Due to the shape of this support boom, support interference effects are larger than the effects of the more slender straight boom. The straight boom however, has no side slip variation possibilities. The choice for the double roll boom is a compromise between test productivity (combining longitudinal and lateral measurements), and elevated support interference effects.

Figure 2: Example of model on rear sting with double roll boom

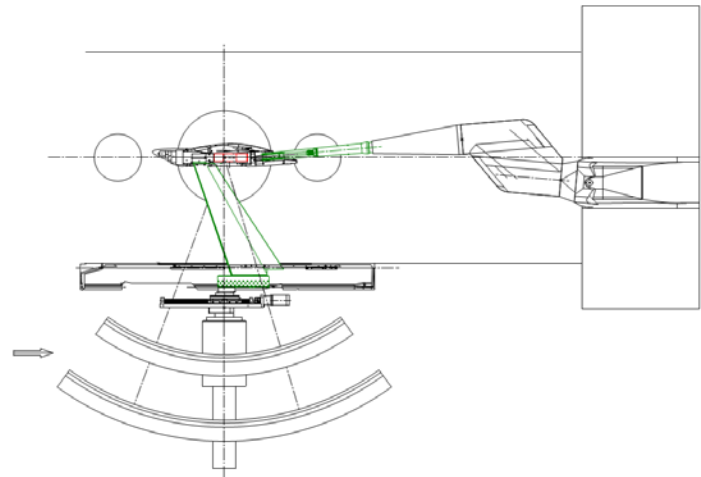


4.2 Dorsal support

The dorsal support is used for support interference assessment investigations (see figure 3). For this purpose, the model is mounted upside down on the dorsal support. Support interference effects are derived from measurements with and without a dummy rear support system. The dummy rear support consists of the double roll boom with straight sting and enters the rear fuselage cavity of the model without mechanical contact. The rotation point of the dorsal support is located at the center

of the main window. This rotation point differs from the rotation point of the rear support. For this purpose, the dorsal support is mounted on a traversing slide to position the model at the same location in the test section as present during the rear support measurements.

Figure 3: Model on dorsal support with dummy rear support



For the configuration with dummy support, a seal is mounted in the model to prevent flow through the model from the dorsal sting cavity to the rear sting cavity. For the configuration without dummy support, the rear cavity is closed with an aft fuselage plug. In the dorsal setup, an angle of attack range between -2 and 6 deg is measured. No side slip measurements are performed.

5 TEST PROGRAM

5.1 Model on rear support

With the model mounted on the rear model support, alpha polars are measured for a range of Mach numbers between Mach numbers 0.5 and 0.83 at a Reynolds number of 3 million. The following model configurations are measured:

- Fuselage only (B)
- Fuselage, wings, pylons and nacelles (WBN)
- Fuselage, wings, pylons and nacelles, horizontal and vertical tail (WBNVH)

The WBNVH configuration is measured in upside-up and upside-down orientation for assessment of the wind tunnel flow up-wash angle. During the rear support test, main balance loads, inclinometer angles, model cavity pressures, model support orientation and tunnel wall pressures are measured.

5.2 Support interference investigations

With the model mounted on the dorsal support, alpha polars are measured for a range of Mach numbers between Mach numbers 0.5 and 0.83 at a Reynolds number of 3 million. The considered model configurations are the same as measured on the rear sting support. Measurements are performed with and without dummy support. During the dorsal support test, the same quantities are measured as during the rear support measurements.

Six parameters are set for each flow condition i.e. the x-position of the model, the angle of attack of the model, the vertical position of the strut, the pitch angle of the rear support, the Mach number and the Reynolds number.

In order to have a good simulation of the support interference effects, the rear sting cavity pressure levels should be the same as measured during the rear model support experiments. During the rear support measurements, the main balance and sting will deflect under the loads on the model. Hence, for each loads case, the position and orientation of the sting in the rear model cavity is different. This affects the interference of the model support on measured drag, lift and pitching moment. The rear cavity pressure and the orientation of the rear model support, as measured during the rear sting support, are used as targets for setting the vertical dummy sting position and orientation of the dummy rear support.

5.3 Empty test section

Test section wall pressures are measured in an empty test section. This is a configuration without wind tunnel model but with the double roll boom in the test section. The empty test section wall pressure data are used for the derivation of wall interference corrections. The Mach number range, alpha range of the model support and the Reynolds number are the same as considered during the rear support measurements (see section 5.1).

6 DATA PROCESSING

6.1 Corrections

Results in this paper are presented for these different correction levels to show the different contributions:

- a) Uncorrected, which means no support or wall interference corrections are applied (“Uncorrected”).
- b) Far field support interference buoyancy correction applied based on test section calibration centerline pressure distribution (“FF SI buoyancy”).
- c) Total support interference correction (“Total SI”) as derived from measurements with and without dummy rear support.
- d) Total support interference correction and wall-induced buoyancy correction applied (“Total SI+WI”).

In the next sections, the different correction levels are discussed in more detail.

6.2 Far field support interference buoyancy correction







In order to understand and analyze support interference effects, it is common practice to consider a breakdown of two interferences. Firstly the far-field interference, which is the overall tunnel flow field disturbance due to the presence of the model support boom in the wind tunnel. As a first estimate, DNW corrects for this effect by a buoyancy type of correction, which acts on the drag component only. This correction is based on the axial pressure gradient determined from tunnel centerline calibrations and the model cross-sectional area distribution. It is well known that the support boom has a significant effect on lift and pitching moment as well.

Secondly there is the near-field correction which is due to the direct effect of the sting on the flow around the model. The sting affects the local pressure field and boundary layer development in the area where the sting enters into the model. In addition, there is a change of local flow directions due to the local flow around the sting-model passage. The latter can cause quite significant effects on lift and pitching moment due to interference on lift-generating surfaces (like the tail plane) and the fuselage after body.

6.3 Total support interference correction

The support interference effect of the total rear support is investigated by using a dummy support entering the rear model cavity model without any contact. In addition, measurements are performed without dummy rear support. An intermediate step is possible where only the dummy sting is removed and the support boom remains in the test section. This enables discriminating between near-field and far-field effects (see figure 4).

Figure 4: Book keeping procedure support interference effects

	C_3	model + dorsal sting + dummy sting + dummy boom
	C_2	model + dorsal sting + dummy boom
Near Field Interference $C_3 - C_2 = \Delta C_{NF}$		dummy sting
	C_2	model + dorsal sting + dummy boom
	C_1	model + dorsal sting
Far Field Interference $C_2 - C_1 = \Delta C_{FF}$		dummy boom
	C_3	model + dorsal sting + dummy sting + dummy boom
	C_1	model + dorsal sting
Total Support Interference $C_3 - C_1 = \Delta C_{SI}$		dummy sting + dummy boom

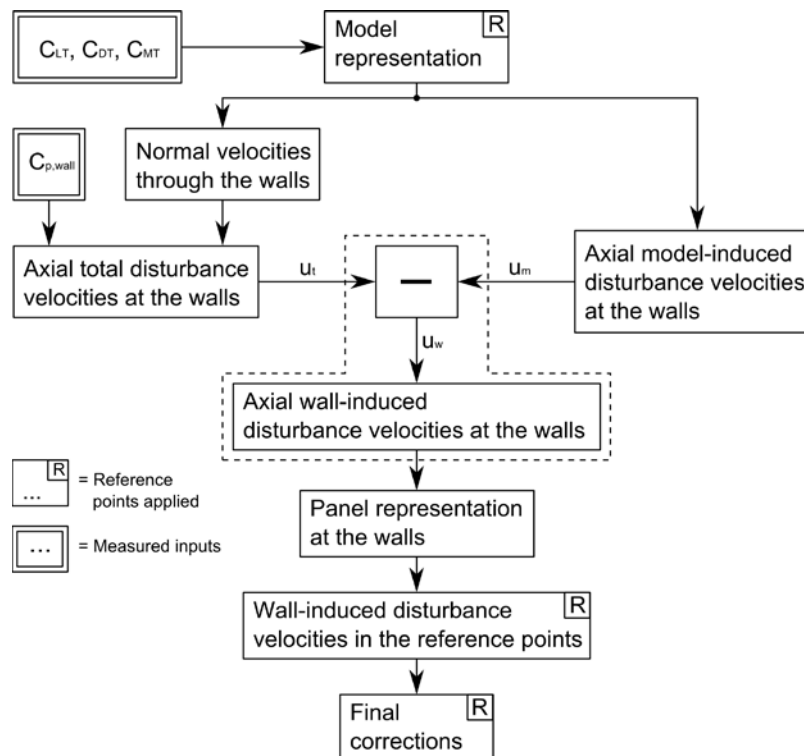
With the complete dummy rear support removed from the test section, there is still a buoyancy effect acting on the model originating from the empty test section (strut and walls). This effect is included in the total support interference correction with a buoyancy correction on drag. There shall be no mutual interference between the dorsal support and dummy rear support. This was confirmed by CFD results performed by NLR.

6.4 Wall interference

A measured wall pressure signature method is used for assessment of wall interferences in the DNW-HST. The method is called WIN3VE and was developed by NLR (see ref. [1]). A schematic flowchart of the method is presented in figure 5. The measured pressures at the walls are affected by flow disturbances from the test section, model support, wind tunnel model and wall interference effects. Wall interference effects of the test section and model support are already included in the test section calibration and support interference correction. Hence, these effects are removed by subtraction of the empty test section wall pressures. The tared wall pressures are used as input for the calculation of the axial total disturbance velocities at the walls by using an estimate of the normal velocities at the ventilated upper and lower wall. The total axial disturbance velocity (U_t) is tared with the direct effect of the model at walls (U_m) by using a simple model configuration (sources, sinks and lifting line theory). The net results (U_w) are the wall-induced axial disturbance velocities at the walls.

A panel calculation method with doublet singularities is used along the wind tunnel walls for calculation of the wall-induced disturbance velocities in the vicinity of the model. The strengths of the doublets are calculated from the axial wall-induced disturbance velocities at the walls (U_w). The wall-induced velocity disturbances in the vicinity of the model serve as input for corrections of angle of attack, Mach number, buoyancy and aerodynamic coefficients according to ref. [1].

Figure 5: Schematic flow chart of wall interference assessment method (WIN3VE)



7 RESULTS

7.1 Up-wash effects

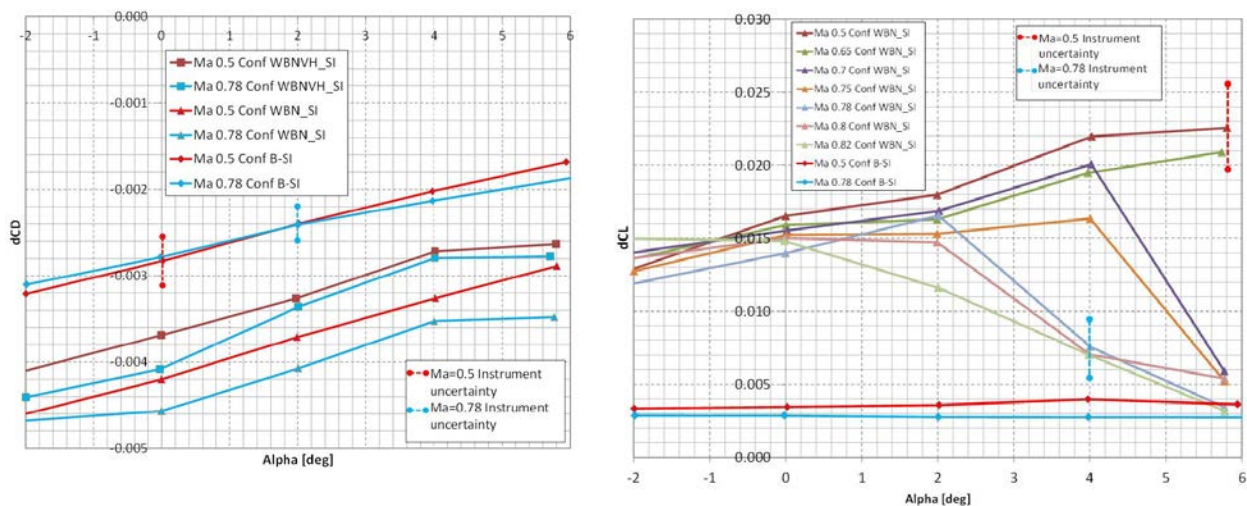
Test section up-wash effects are derived from a comparison of lift versus alpha curves for model- and support-oriented, normal and inverted (not presented). The assumption is that differences in lift curves are only due to test section flow up-wash effects. In reality, differences are also affected by measurement errors in alpha, dynamic pressure and lift force. The observed up-wash angle is in the order of only 0.01 deg, which might also be due to an error in the lift coefficient of 0.002. From a main balance repeatability point of view, an error of 0.002 in the lift coefficient is a realistic value. Hence, no up-wash correction is applied.

7.2 Support interference effects

All corrections presented in this paragraph should be subtracted from the measured drag, lift and pitching moment coefficients. Figure 6 presents the total support interference corrections for drag and lift

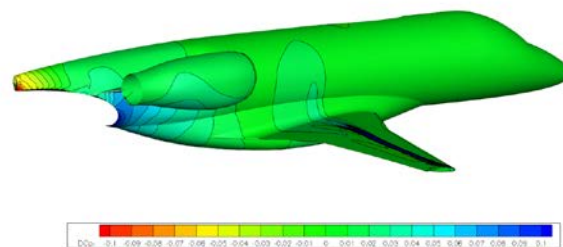
coefficients versus alpha for different Mach numbers. Total support interference levels on drag are between 0.0016 and 0.0047 depending on the model configuration, angle of attack and Mach number. A linear effect with alpha is visible for the fuselage only (B) results. The effect of Mach number is limited to 0.0002. The trends for configurations WBN and WBNVH are similar at corresponding Mach numbers, with the lower drag effects for the complete configuration. Near- and far-field effects on drag are for all configurations of the same order of magnitude (not presented). Support interference corrections are derived from measurements with and without dummy rear support. Hence, the uncertainty in the corrections should be within the repeatability margin of the main balance which is in the order of $\pm 0.1\%$ of the full scale. The repeatability margins are presented in figure 6.

Figure 6: Total support interference for model configurations WBNVH, WBN and B at different Mach numbers. Left: Drag coefficient; Right: Lift coefficient



For lift, the support interference levels are between 0.003 and 0.025 depending on the configuration. Corrections in the order of 0.003 are necessary for configuration fuselage only. Variation with Mach number and alpha is limited. Results for configuration WBNVH are not presented due to the strong resemblance with the WBN results.

Figure 7: Surface pressure increments due to the rear support calculated with CFD by NLR (Ma=0.78)



For low Mach numbers, a linear trend with alpha is observed. For higher Mach numbers, support interference is not linear with angle of attack. A kink is visible in the curves, appearing at lower angles of attack for increasing Mach numbers. This effect is attributed to support interference effects acting at the

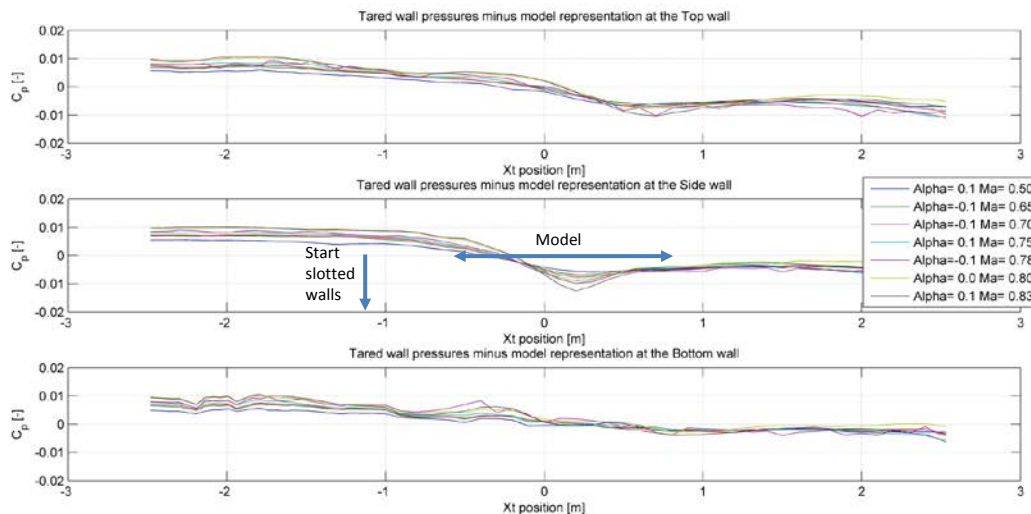
wing location. From CFD calculations performed by NLR, it appears that the effect of the rear support is limited to the aft fuselage region at Mach number 0.5. For increasing Mach numbers, the effect is extended to the wing region. The wing features a shock wave and associated recompression region which is sensitive to small shifts in the local Mach number. The rear support has an effect on the position of the shock introducing a loss in lift (see figure 7). The kink in the curves can be traced back to mainly originating from far field effects and is not visible in the drag and pitching moment support interference corrections.

Support interference effects on the pitching moment are almost constant with angle of attack and Mach number. Levels for configurations B, WBN and WBNVH are -0.006, -0.024 and -0.036, respectively.

7.3 Wall interference effects

Figure 8 presents the wall-induced pressure signature at the walls of the DNW-HST for varying Mach numbers at zero angle of attack. The effects of the model support and the model are subtracted. Results are provided along the centerlines of the upper, side and lower wall. The MRP of the model is located at $X_T = 0.05$ m. As can be observed at all walls, the pressure coefficients are close to zero at the model MRP. From this figure it can be concluded that the wall interference has a limited effect on the Mach number at the model MRP ($\Delta Ma \sim 0.001$).

Figure 8: Wall-induced pressures at upper, side and lower walls for configuration WBNVH at alpha ~0 deg and varying Mach numbers

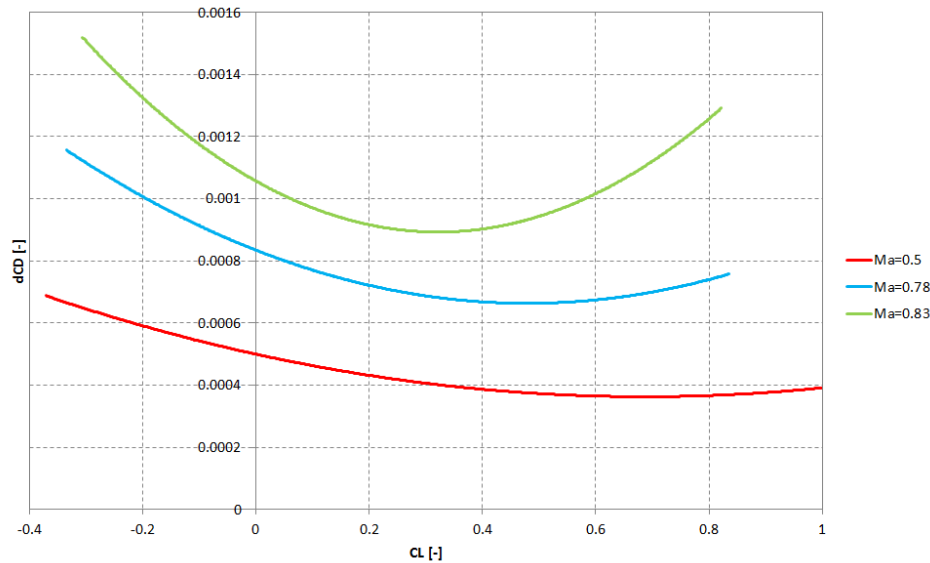


The figure shows a non-zero C_p level upstream of the slotted test section. The C_p level appears to be dependent on the Mach number and the angle of attack. This is an indication that the ventilated walls do not compensate entirely for the blockage effect. With C_p levels almost zero at the model MRP, the model experiences a wall-induced pressure gradient pushing the model downstream. Hence, wall-induced buoyancy effects result in an increase in measured drag where support interference effects have the opposite effect. This confirms the hypothesis that was addressed in the introduction.

Figure 9 shows the wall-induced buoyancy effect as function of CL for different Mach numbers. The wall-induced buoyancy is dependent on CL and Mach number and hence, will have an effect of drag creep curves. Wall-induced angle of attack effects are in the order of -0.04 to 0.04 deg depending on the lift.

For this test, DNW only corrects the data for total support interference effects and the wall-induced buoyancy. Wall-induced effects on angle of attack and Mach number are so small that a sound validation of these corrections are not available yet and hence, are not corrected for.

Figure 9: Wall-induced buoyancy levels as function of CL for different Mach numbers. Model configuration: WBN



7.4 Verification of results

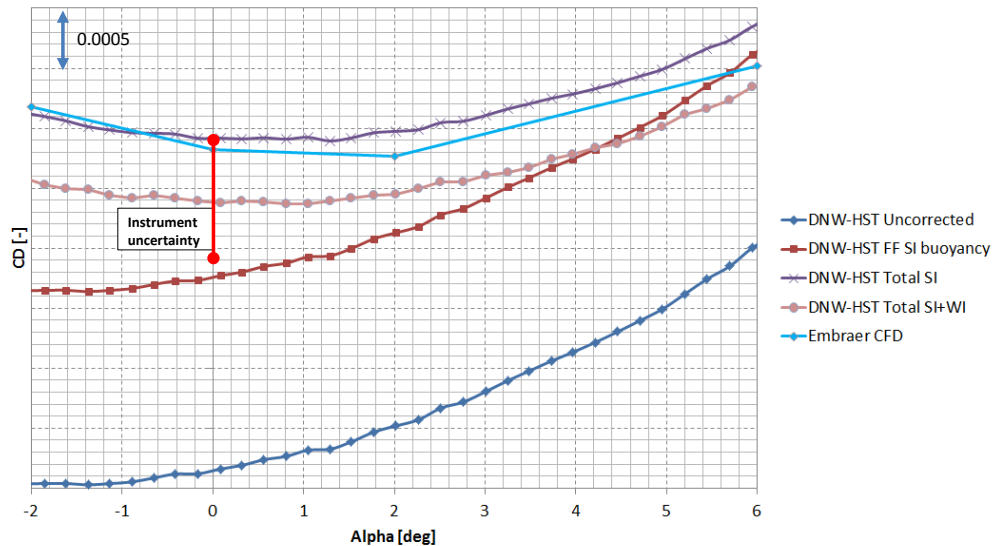
Results are presented for the model configurations body-alone and WBN separately. Axis labels have been removed for confidentiality reasons.

Body-alone configuration

For the body-alone configuration, CFD data from Embraer is available to verify the results. For body-alone, only support interference and blockage effects have an effect on the flow field. Figure 10 presents the experimental drag coefficient versus alpha for different correction levels in comparison to CFD results for Mach number 0.78. From a comparison with the uncorrected data, it can be concluded that the total support interference correction is the main correction term. The figure shows that the drag curve rotates after correction for total support interference. The trend of the curve is similar as for the CFD results. Drag levels are in the order of 0.0002 larger than the CFD results. After additional correction of the wall-induced buoyancy, the drag levels are reduced. The fully corrected experimental drag results are in the order of 0.0004 lower than the CFD result, which is in the order of the instrument uncertainty. For transonic conditions ($Ma > 0.7$), the uncertainty in CFD drag calculations is in the order of ± 0.0003 .

For the lift and pitching moment coefficients, the maximum differences between CFD and fully corrected experimental data are respectively 0.002 and 0.002 which is also within the instrument uncertainty. Similar differences are present at other Mach numbers.

Figure 10: Comparison of numerical and experimental data for drag versus alpha at Ma=0.78 and configuration body-alone



Configuration WBN

Figure 11 shows a comparison between measured results in DNW-HST with results from ETW and CFD. Comparison of the DNW-HST lift versus alpha results with ETW results shows that the curves are running parallel for attached flow regimes. The maximum difference in the lift coefficient is 0.005. These are differences that are within the instrument uncertainty limits. The behavior in separated flow areas is somewhat different. CFD lift coefficient results are larger than the experimental results in DNW-HST and ETW (~0.03 at CLO). CFD tends to over predict the lift coefficient for zero angle of attack in comparison to wind tunnel data. This coefficient is closely related to the development of the boundary layer, mainly, over the wing. For medium Reynolds numbers (3 million), the simulated boundary tends to be slightly thinner in comparison to the wind tunnel data, which explains the higher CLO. The main contributors for this are:

- Turbulence model accuracy for medium Reynolds.
- CFD mesh quality, especially at leading edges.

These factors combined can lead to differences in the order of 0.03 in lift coefficient, which is of the same order of magnitude as the observed differences. The observed differences between the experimental and CFD results increase with increasing lift values. This might be due to wing deformation effects in the experimental results. Experimental wing deformation results in lower local effective angles of attack for positive wing loads i.e. nose down wing tip twist.

The right plot of figure 11 shows the drag versus lift for different data processing steps. Drag levels are subtracted with the ideal induced drag to facilitate data comparison. The figure shows DNW-HST data at different correction levels. By correcting for support interference, the results show an increase in drag. By addition of the correction for wall interference, the drag levels are reduced, bringing the fully corrected results in close agreement with the ETW results. By comparing with the ETW results, it is concluded that maximum differences in drag between DNW-HST and ETW are about 0.0005 comparable with the instrument uncertainty. CFD results in this plot seem to be shifted in lift direction with respect to the experimental data as was observed as well in the lift polars. A shift in lift of about 0.03 to lower values would result in a better agreement with experimental data for drag as well.

Figure 11: Comparison of numerical and experimental data at Ma=0.78 and configuration WBN; Left: CL-alpha; Right: CL-CDNET

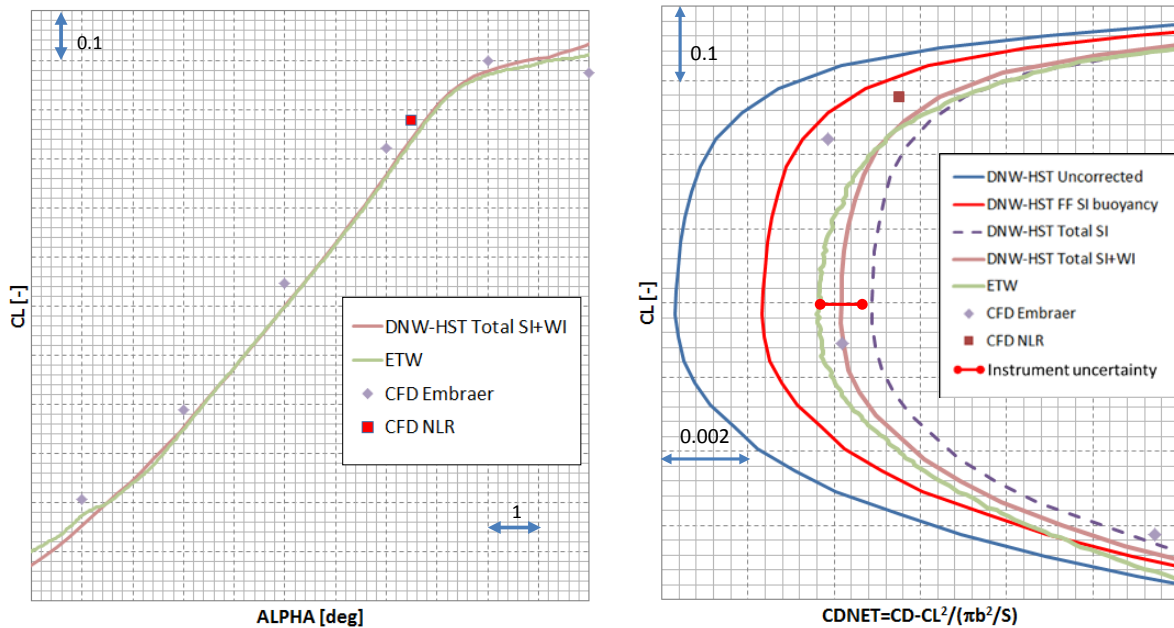
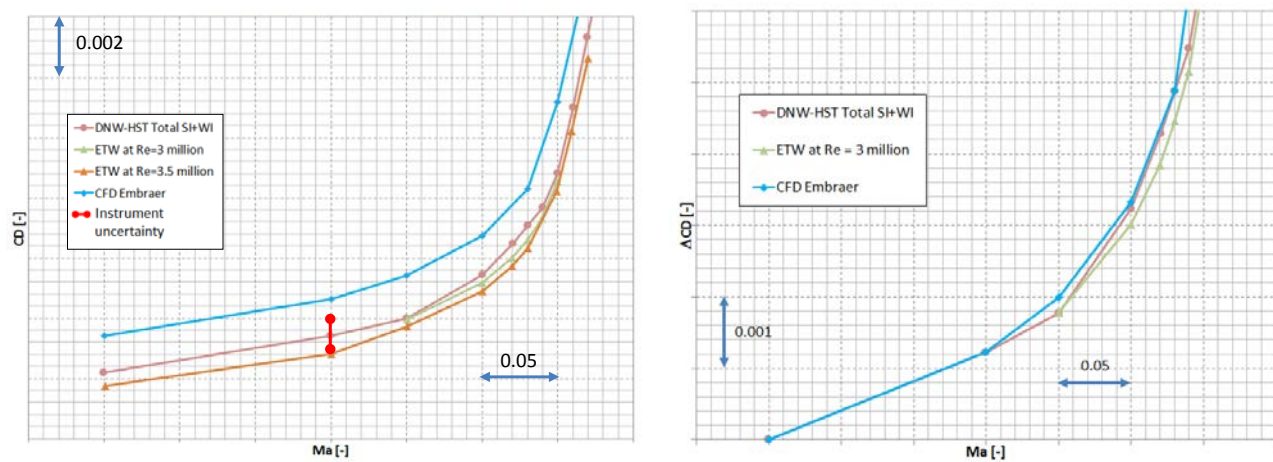


Figure 12 shows the absolute drag versus Mach number at $\alpha=2$ deg for configuration WBN. The figure shows results for DNW-HST (Total SI+WI), ETW for two Reynolds numbers and CFD results from Embraer.

Figure 12: Comparison of numerical and experimental drag versus Mach number for configuration WBN at $\alpha=2$ deg and $Re=3$ million unless stated otherwise. Left: absolute drag; Right: relative drag



Differences in drag between DNW-HST results and ETW at Reynolds number of 3 million are between 0 and 0.0004 depending on the Mach number. Drag levels at Reynolds number of 3.5 million are expected to be in the order of 0.0004 lower than at 3 million. CFD drag results are in the order of 0.0012 larger than the experimental results. The increase of drag as function of Mach number (drag creep) is within 0.0002 in agreement for the experimental DNW-HST results and the CFD results (right plot of figure 12).

8 CONCLUSIONS AND OUTLOOK

With the introduction of a wall-induced buoyancy correction, drag levels are reduced in DNW-HST. The hypothesis that a wall-induced pressure gradient pushes the model downstream is proven. Verification with data measured in the ETW, shows agreement on drag and lift within the instrument uncertainty limits. The increase of drag as function of Mach number (drag creep) is within 0.0002 in agreement for the experimental DNW-HST results and the Embraer CFD results. Based on these results, it is concluded that high data quality is ensured in the DNW-HST wind tunnel.

Differences in lift are observed between the experimental results (DNW-HST and ETW) and the CFD results. The differences might be due to inaccuracies in the CFD turbulence model and mesh quality and are an order of magnitude more significant than the instrument uncertainties. Remaining lift dependent differences might be explained from wing deformation effects.

For this investigation, a main balance with uncertainty of $\pm 0.3\%$ of the full scale was used. Introduction of new internal main balances with reduced uncertainty and improved repeatability will reduce the uncertainty in the support interference corrections as well as the overall measurement accuracy. DNW has purchased several new balances with improved uncertainty limits. The aim is to reduce the instrument uncertainty to $\pm 0.1\%$ of the full scale.

On request of DNW, NLR is working on a CFD model of the DNW-HST to investigate wall interference effects. The aim is that this CFD model can be used to verify the wall interference corrections as provided by the measured wall pressure signature method (WIN3VE) of DNW.

Wing deformation has an effect on the measured lift values. This deformation is measured with optical Stereo Pattern Recognition (SPR) techniques in the DNW wind tunnels. The SPR results are used as input for CFD calculations with deformed wings. Embraer and DNW are cooperating to further understand the effect of wing deformation on the test results.

In order to quantify and qualify results from different wind tunnels facilities, Embraer is working on a Transonic Research Reference Model. Each transonic wind tunnel has its own characteristics and, consequently, its own wind tunnel corrections. In most of the cases, aircraft manufacturers find considerable different absolute values for the same wind tunnel model geometry when testing in different wind tunnel facilities. The differences sometimes can be so high that wrong transonic design conclusions can be taken, depending on where the test is performed. Possible causes for differences are balance/instrumentation uncertainties, Reynolds effects, test procedures and adopted wind tunnel correction procedures. But having only those arguments, it is not sufficient enough to solve the main question: "Are reliable corrected absolute data acquired"? Hence, in order to have this question solved, Embraer is considering designing and manufacturing a new transonic reference model (with aerodynamics previously validated). A standard research and development test is performed in cooperation with several transonic wind tunnel partners to finally reach valuable transonic comparable conclusions.

9 ACKNOWLEDGEMENT

The authors are indebted to Rodrigo Felix of Embraer for providing CFD results and his valuable comments during the execution of this cooperative project. Also Roy Gebbink from DNW is thanked for his critical reviews of this project.

10 REFERENCES

- [1] Labrujère, Th. E.; Maarsingh, R. A.; Smith, J.; "Evaluation of Measured-Boundary-Condition methods for 3D subsonic wall interference", NLR Technical report TR 88072 U, 1988